Research Article

Journal of Applied Toxicology

Received: 29 January 2014, Revised: 27 March 2014, Accepted: 1 April 2014 Published online in Wiley Online Library: 12 September 2014

(wileyonlinelibrary.com) DOI 10.1002/jat.3024

Graphene supports *in vitro* proliferation and osteogenic differentiation of goat adult mesenchymal stem cells: potential for bone tissue engineering

Hoda Elkhenany[a], Lisa Amelse[a], Andersen Lafont[b], Shawn Bourdo[b], Marc Caldwell[a], Nancy Neilsen[a], Enkeleda Dervishi[b], Oshin Derek[b], Alexandru S. Biris[b], David Anderson[a] and Madhu Dhar[a]*

ABSTRACT: Current treatments for bone loss injuries involve autologous and allogenic bone grafts, metal alloys and ceramics. Although these therapies have proved useful, they suffer from inherent challenges, and hence, an adequate bone replacement therapy has not yet been found. We hypothesize that graphene may be a useful nanoscaffold for mesenchymal stem cells and will promote proliferation and differentiation into bone progenitor cells. In this study, we evaluate graphene, a biocompatible inert nanomaterial, for its effect on *in vitro* growth and differentiation of goat adult mesenchymal stem cells. Cell proliferation and differentiation are compared between polystyrene-coated tissue culture plates and graphene-coated plates. Graphitic materials are cytocompatible and support cell adhesion and proliferation. Importantly, cells seeded on to oxidized graphene films undergo osteogenic differentiation in fetal bovine serum-containing medium without the addition of any glucocorticoid or specific growth factors. These findings support graphene's potential to act as an osteoinducer and a vehicle to deliver mesenchymal stem cells, and suggest that the combination of graphene and goat mesenchymal stem cells provides a promising construct for bone tissue engineering. Copyright © 2014 John Wiley & Sons, Ltd.

Keywords: Goat mesenchymal stem cells; oxidized graphene; bio-scaffold; osteogenesis

Introduction

Annually, victims of severe musculoskeletal injury suffer skeletal bone defects requiring extensive surgery, prolonged convalescence and, in many cases, amputation. In an attempt to improve outcomes and speed recovery, bone tissue engineering and regenerative medicine research have markedly increased (Mistry and Mikos, 2005; Nandi *et al*., 2010; Salgado *et al*., 2004). Features central to bone tissue engineering include a scaffold, viable cells and/or biologically active molecules in combinations suitable for implantable composite constructs. Scaffolds must be biocompatible and should be biomimetic for the intrinsic characteristics of bone. Ideally, these components are replaced over time by the patient's tissues resulting in complete restoration of normal form and function. Nanomaterials have emerged as promising components of scaffolds owing to their potential to imitate the natural extracellular matrix and to replace damaged bone tissues efficiently (Biswas *et al*., 2012; Zhao *et al*., 2013).

Recently, graphene has been recognized as a biomimetic nanomaterial and has been proposed for a number of biomedical applications (Mahmood *et al*., 2013; Nayak *et al*., 2010, 2011). Graphenes represent a novel form of carbon lattice having a 2-D structure and are amenable to building complex structures. The carbon atoms forming graphene provide the basis for its enhancement with both positive and negative functional groups. Graphene has excellent mechanical properties (high elasticity, strength, flexibility) and can be tailored for various functionalities on flat surfaces (Lee *et al*., 2008). It also has the potential to be used as a reinforcement material in hydrogels, biodegradable films, electrospun fibers and other tissue engineering scaffolds (Dervishi *et al*., 2013; Pruneanu *et al*., 2012; Zhang *et al*., 2011). Graphene-based biomaterials have been demonstrated to support proliferation of human mesenchymal stem cells (MSCs) and promote osteogenic and cardiomyogenic differentiation, *in vitro* (Nayak *et al*., 2010, 2011; Park *et al*., 2013). We have recently reported that carboxylated multiwalled carbon nanotubes and carboxylated graphenes can stimulate osteogenic differentiation *in vitro*, in mouse osteoblastic cell line, MC3T3-E1, and significantly increase the amount of bone mineral formation (Mahmood *et al*., 2013). Additionally, surface coating of Si/SiO_2 chips with graphene sheets has been shown to accelerate the differentiation of human MSCs into osteoblasts and enhance mineral deposition despite the lack of an increase in growth rate *in vitro* (Nayak *et al*., 2010, 2011). In contrast, another report has

*Correspondence to: M. Dhar, Department of Large Animal Clinical Sciences, University of Tennessee, Knoxville, TN 37996, USA.
Email: mdhar@utk.edu

[a]Department of Large Animal Clinical Sciences, University of Tennessee, Knoxville, TN, 37996, USA

[b]The Center for Integrative Nanotechnology Sciences, University of Arkansas, Little Rock, AR, 72204-1099, USA

shown that graphene inhibited cell proliferation, osteogenic differentiation and mineralization of rat MSCs *in vitro* (Liu *et al.*, 2010). Data from these published studies demonstrate that further research is needed regarding the potential applicability of graphene and graphene oxide sheets as biocompatible, transferable and implantable platforms for stem cell culture and delivery.

Stem cell-based therapies present special challenges that will require the development of new protocols and test systems, before being translated for clinical use in humans. Bone marrow-derived MSCs (BMMSCs) are ideally suited for bone tissue engineering applications. BMMSCs are desirable because of their capabilities for self-renewal and osteogenic differentiation potential both *in vitro* and *in vivo* (Bruder *et al.*, 1997; Jaiswal *et al.*, 1997). Animal species, such as rabbits, dogs, pigs, sheep, goats and non-human primates, may be useful as predictors of responses in humans and offer advantages over rodents for preclinical testing (Harding *et al.*, 2013). Goats are commonly used as large animal models for orthopedic therapies (Murphy *et al.*, 2003; Tang *et al.*, 2007).

We hypothesized that graphene films would promote cell proliferation and enhance osteogenesis of goat BMMSCs with the potential to be used as an implantable scaffold in subsequent studies of bone defects. Before being translated into clinical practice, it is necessary to assess the effects of graphene, if any, on cell proliferation and differentiation of BMMSCs, *in vitro*. The objectives of the present study were to isolate and characterize goat BMMSCs (caprine, cBMMSCs); establish cell culture lines of cBMMSCs; and to evaluate the rate of cell proliferation and osteogenic differentiation of cBMMSCs on regular polystyrene-coated tissue culture (TCP) and oxidized graphene (GO) sheets *in vitro*. We propose that, given its unique biochemical properties, graphene could become building block material for the complex construction of biomimetic structures that could be used successfully for clinical applications of tissue regeneration.

Materials and Methods

Media and Chemicals

All chemicals, cell culture supplements and disposable tissue culture supplies were purchased from Fisher Scientific (Pittsburgh, PA, USA) unless otherwise noted. Animal experimental procedures were carried out according to the Institutional Animal Care and Use Committee (protocol no. 5027).

Treatment of Tissue Culture Plates with Graphene

Commercially purchased graphene sheets (Angstrom Materials Inc., Dayton, OH) were oxidized using a 3: 1: 1 ratio mixture of sulfuric acid, nitric acid and deionized water, and then vacuum filtered through 0.2 μm GTTP Millipore membranes (EMD Millipore Corporation, Billerica, MA, USA). The GO was then washed using deionized water until all the acid was removed (pH neutral). GO was characterized using thermogravimetric analysis, as well as scanning electron microscopy (SEM), atomic force microscopy (AFM) and transmission electron microscopy (TEM). The GO was dispersed in deionized water (0.1 mg ml^{-1}) and then air-sprayed on to tissue culture dishes (20 ml solution/one 6- or 24-well dish). To evaluate thickness of the graphene films, a similar spray deposition was performed where glass (for AFM) and silicon (for SEM) substrates were placed in some of the wells of a tissue culture dish and the resulting graphene films were analyzed.

Characterization of Graphitic Materials

SEM analysis was performed using a field emission SEM, JSM-7000 F (JEOL USA, Inc. Peabody, MA.). Powder graphene samples were placed on double-sided carbon tape (Fisher; 8MM, cat. no.: 50-285-81) using a disposable spatula (VWR International; Radnor, PA; cat no.: 80081–194) and were attached to aluminum stubs. Silicon substrates were placed perpendicularly on aluminum stubs so that the edge could be analyzed for film thickness and uniformity. The accelerating voltage was set at 15 kV and the working distance at 10 mm. TEM analyses were performed using a JEOL field emission TEM (model JEM-2100 F) equipped with a pair of charge-coupled device cameras. High-resolution images were taken at 80 kV. AFM was performed using a Veeco Dimension 3100 (ClassOne Equipment Inc., Atlanta, GA); glass substrates were analyzed for thickness measurements by removing part of the graphene film with a razor blade and then analyzing the step height of the graphene/glass interface.

Harvesting and Isolation of Caprine Mesenchymal Stem Cells

Adult MSCs were obtained by centrifugation of bone marrow aspirated from the sternum of two healthy 2–5-year-old mixed breed goats according to methods described earlier (Carter-Arnold *et al.*, 2013; Favi *et al.*, 2013; Nair *et al.*, 2009; Ren *et al.*, 2012). Briefly, animals were sedated, and the sternum was aseptically prepared. Bone marrow aspirates were collected in the presence of 300 U ml^{-1} of heparin, diluted 1: 4 with phosphate-buffered saline, pH 7.4 (PBS), layered over 15 ml of Ficoll, and centrifuged for 20 min at 400 *g*. The cells at the interface of the PBS and Ficoll containing the mononuclear fraction were aspirated and washed in PBS by centrifuging for 10 min at 200 *g*. The supernatant was aspirated, and the cell pellet was resuspended and plated on tissue culture dishes in Dulbecco's modified Eagle medium F-12 containing 10% fetal bovine serum (Hyclone, Logan, UT, USA) and 1% penicillin/streptomycin solution in a 37 °C, 5% CO_2 incubator (passage 0). This is the complete growth medium. Adherent cells were allowed to reach 70% confluency before harvesting by treatment with 0.25% trypsin and re-plated for further expansion (passage 1). At the end of the second passage, caprine MSCs (cMSCs) were banked in liquid nitrogen in cryopreservation medium (50% fetal bovine serum, 5% dimethyl sulfoxide, 45% Dulbecco's modified Eagle medium F-12).

Low passaged cells (passages 2–4) were used in all the experiments except in the CFU assay. In the CFU assay, we used freshly isolated mononuclear cells (passage 0) and one high passage (passage 7).

Colony-Forming Unit Assays

Roughly, 4×10^6 freshly isolated mononuclear cells purified from bone marrow aspirates and 100 cBMMSCs of passage 7 were plated on to 100 mm tissue culture dishes. After incubation for 6 days in a 37 °C, 5% CO_2 incubator, cells were washed with PBS and fixed with 10% formalin for 10 min at room temperature. Subsequently, the colonies were stained with 0.5% crystal violet solution for 5 min at room temperature. Images were obtained using a Zeiss Axiovert 40C microscope, equipped with a Canon, Powershot A620 camera.

Journal of Applied Toxicology

RNA Isolation and Real-Time Polymerase Chain Reaction

RNA isolation and real-time quantitative polymerase chain reaction (PCR) from undifferentiated cBMMSCs were performed as described earlier (Carter-Arnold *et al*., 2013). Total RNA was extracted from a minimum of 2.0×10^5 proliferating cells using an RNeasy Mini RNA kit (Qiagen, Valencia, CA, USA) according to the manufacturer's instructions. Briefly, 2.0×10^5 cells yielded 100–500 $\mu g\,ml^{-1}$ of total RNA. One microgram of total RNA was reverse-transcribed in a 10 μl reaction volume for cDNA synthesis (BioRad, Hercules, CA, USA). Quantitative PCR to assess the expression of caprine-specific mRNAs for CD29, CD45 and CD90 was carried out using SYBR green-based absolute blue quantitative PCR mix. One hundred pM of each forward and reverse primer mix was used. Gene-specific primer sequences were deduced from published reports (Ren *et al*., 2012) and were commercially obtained. Each real-time PCR product was analyzed and confirmed for its size using neutral 1–1.5% agarose gel electrophoresis.

Trilineage Differentiation Assays

Osteogenesis, chondrogenesis and adipogenesis were performed on six-well TCP plates as described earlier with slight modifications (Carter-Arnold *et al*., 2013; Favi *et al*., 2013). Cells (2×10^5) were seeded in complete growth media, and 48 h later, when cells were 70% confluent, lineage-specific differentiation was induced. Cells were fed with the specific differentiation media throughout the differentiation process and media was replenished every 3 days. For each differentiation assay, an identical number of non-induced cells (cells without any differentiation media) were used as controls.

Osteogenic differentiation was induced in complete growth medium supplemented with 1 nM dexamethasone, 20 mM β-glycerophosphate and 50 μM ascorbic acid, and differentiation was monitored using alizarin red staining at 21 days.

Chondrogenic differentiation was induced in complete growth medium supplemented with 100 nM dexamethasone, 0.25 mM ascorbic acid and 5 $ng\,ml^{-1}$ transforming growth factor β1, and differentiation was monitored using alcian blue staining at 14 days.

Adipogenic differentiation was induced in complete growth medium supplemented with 1 μM dexamethasone, 10 $\mu g\,ml^{-1}$ recombinant human insulin, 0.5 mM 3-isobutyl-1-methylxanthine, 15% rabbit serum and 20 μM indomethacin, and differentiation was monitored using oil-red-O staining at 14 days. All staining images were taken with a Zeiss Axiovert 40C microscope, equipped with a Canon, Powershot A620 camera and analyzed using ZoomBrowser EX software.

Goat BMMSCs were seeded and assayed on GO plates using identical passages and media as described for TCP. Cell numbers found optimal in the proliferation assay were seeded in complete growth media described above and subjected to osteogenesis when they were 70% confluent. The medium was changed every 3 days, and all assays were carried out simultaneously on TCP and GO plates.

Cell Adhesion and Viability Assays

Cell viability was measured after 2, 7 and 10 days using the CellTiter 96® Aqueous Non-Radioactive (MTS) assay (Promega,

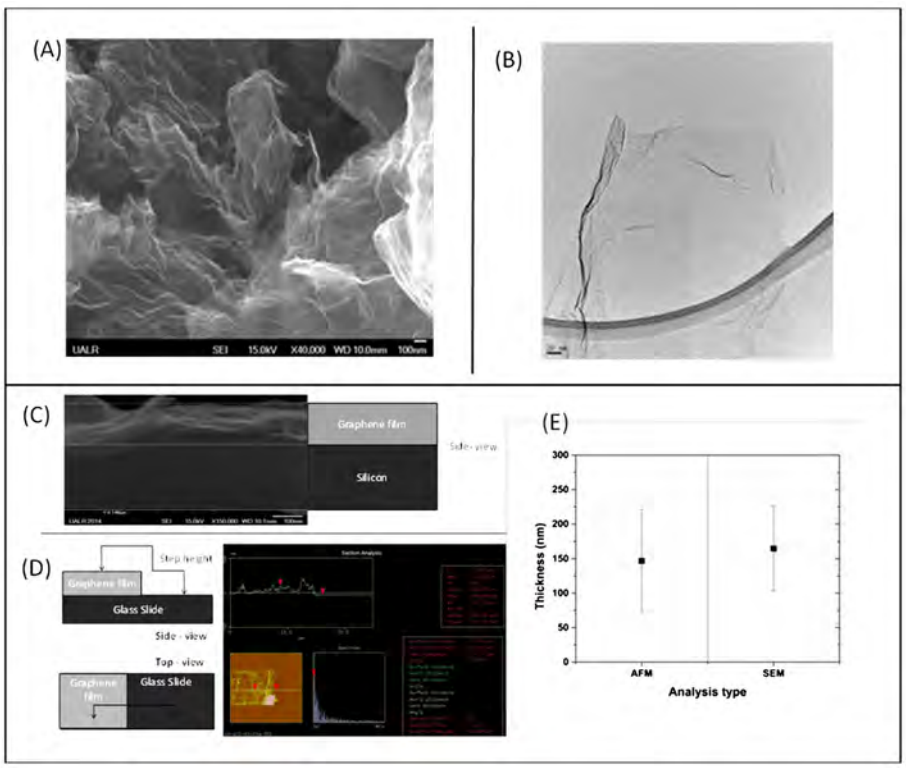

Figure 1. Representative imaging for oxidized graphene characterization: (A) SEM image of oxidized graphene powder; (B) transmission electron microscopy image of oxidized graphene powder; (C) representative side view of SEM image of oxidized graphene/silicon interface for thickness measurement, including schematic to identify silicon and oxidized graphene interface; (D) AFM analysis for thickness measurement showing both side and top views, including schematics to identify glass and oxidized graphene interface and (E) graphical results from AFM and SEM thickness analysis (average 30 sections over six sample areas for AFM and average of seven SEM images). AFM, atomic force microscopy; SEM, scanning electron microscopy.

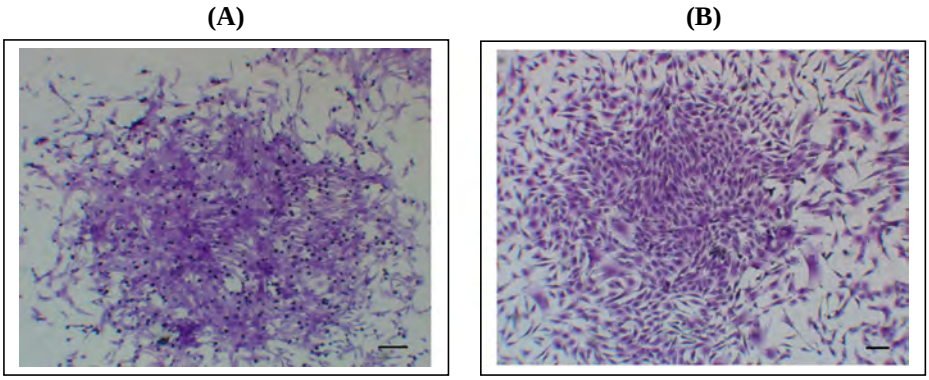

Figure 2. A representative photograph of colony forming assay of (A) freshly isolated bone marrow-derived mononuclear cells (passage 0) and of (B) bone marrow-derived mesenchymal stem cells (passage 7). Clusters of colonies were visualized by crystal violet staining. Scale bar = 100 μm.

Madison, WI, USA) according to the manufacturer's instructions. All experiments were simultaneously conducted in triplicate on 24-well TCP and GO scaffolds. Four different cell densities (1×10^3, 5×10^3, 10×10^3 and 20×10^3 cells) were used. Cells were incubated for 2, 7 and 10 days in growth media at 37 °C, 5% CO_2. For quantitation, MTS reagent in a 5: 1 ratio was added to each well and incubated for 3 h at 37 °C, 5% CO_2. Then, samples ($n = 4$) were transferred to 96-well plates, and the optical density was measured on a microplate fluorescence reader (BioTek, Winooski, VT, USA) using an absorbance of 490 nm. Non-seeded TCP and GO scaffolds in the same media were used as blanks. The respective blank readings were subtracted from the values at 490 nm to yield the corrected absorbance.

Cell adhesion and viability was microscopically assessed after 2, 7 and 10 days using calcein-AM (Invitrogen, Eugene, OR, USA) and propidium iodide (Invitrogen, Carlsbad, CA, USA). Optimal numbers of goat BMMSCs were seeded on TCP and GO plates at a density of 1.0×10^3 cells per well in a 24-well plate.

Cells were stained according to the manufacturer's protocols and subsequently visualized using a Zeiss Axiovert 40C microscope (Carl Zeiss MicroImaging, Inc., Thornwood, NY, USA) equipped with a Nikon Digital Sight DS-Qi1Mc camera (Nikon Instruments Inc., Melville, NY, USA).

Osteogenesis Quantification Assay

Osteogenesis was quantitated using a commercially available osteogenesis assay kit according to instructions. Roughly, 2×10^4 cells were seeded on to 24-well plates and induced towards osteogenic differentiation. For the osteogenesis quantification, the cells were first stained with alizarin red, then 400 μl of 10% acetic acid was added to each well, and cells were incubated at room temperature for 20 min. The cells were harvested by scraping and were heated to 85 °C for 10 min. After being cooled on ice for 5 min, the samples were centrifuged to remove any cell debris. Roughly, 350 μl of supernatant were carefully removed and neutralized with 150 μl 10% ammonium hydroxide solution. One hundred μl of each sample ($n = 6$) were transferred on to a 96-well plate, and the optical density was measured on a microplate fluorescence reader (BioTek) using an absorbance of 405 nm. High (31.3 μM–2 mM) and low (0.47 M–30 μM) range standards were used for extrapolation and calculation of alizarin red concentration in each sample.

Statistical Analysis

All experiments were carried out with $n = 3$–12 samples and data were expressed as mean ± SD of at least three independent samples. Statistical comparisons between groups were performed with a two-tailed Student's *t*-test; $P < 0.05$ was considered significant.

Results and Discussion

Graphene-Coated Plates

The TEM and the SEM analyses of the individual graphitic structures (composed of two to three graphitic layers and a surface area of 589.04 ± 2.6 $m^2\,g^{-1}$) used in this study are shown in Fig. 1. The graphene solution was then air-sprayed into thin films inside the petri dishes. After coating TCP plates with 0.1 mg ml^{-1} graphene by air spraying, each film preparation was checked for its uniformity in thickness and integrity using visual inspection. A separate spray deposition, in which glass and silicon substrates were placed in the TCP wells for post-deposition characterization, was performed in the same manner as the TCP for cell growth studies. For thickness determination by AFM, six different graphene/glass interface areas were investigated and step height was determined by analyzing various cross-section slices of each area (30 total data points). For SEM, a silicon wafer was used as a conductive substrate so charging would not occur during the electron bombardment of the specimen. The substrate was oriented normal to the beam so that the edge could be seen and a thickness could be determined (seven total images analyzed). After image collection and analysis, the averages from both SEM and AFM were determined to be 147 ± 74 nm and 165 ± 61 nm, respectively. While the errors seem large, this can be attributed to areas that graphene flakes are not laying "flat" and therefore increase the apparent thickness of the film.

Characterization of Goat Adult Mesenchymal Stem Cells

The isolated cBMMSCs were characterized to ensure that they satisfied the three important criteria used to identify MSCs (Dominici *et al.*, 2006; Pittenger *et al.*, 1999). These included their ability to adhere to TCP, proliferate as a cluster of colonies (CFU), express specific surface antigens and demonstrate the potential to differentiate into lineages of mesenchymal tissues.

Journal of Applied Toxicology

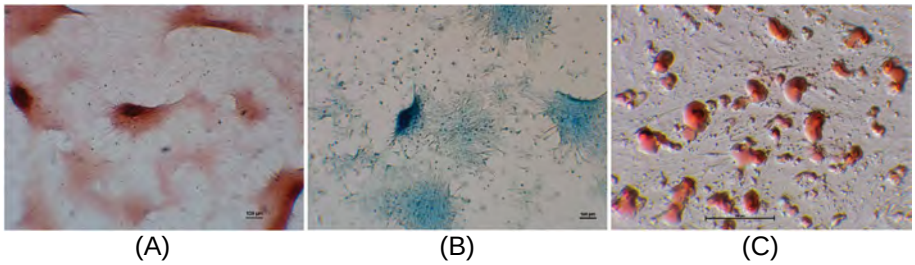

Figure 3. Trilineage differentiation assays of caprine bone marrow-derived mononuclear cells. Representative images showing alizarin red (A), alcian blue (B) and oil-red-O (C) staining, of osteocytes, chondrocytes and adipocytes, respectively, after *in vitro* differentiation. Cell-specific staining is detected at 21, 14 and 14 days post-differentiation, respectively. Scale bar = 100 μm. Adipocytes are photographed at × 20 magnification for easy visualization.

Primary adherent cell cultures were generated from bone marrow samples harvested from two goats. Cells displayed an MSC-like phenotype on TCP. As judged by crystal violet staining, after 6 days in culture, roughly 4×10^6 freshly isolated mononuclear cells from bone marrow aspirates formed 200–250 clusters of colonies representing CFUs (Fig. 2A). Each cluster of confluent MSCs exhibited fibroblast-like typical MSC morphology. Confluent cells at this stage were successfully passaged, and goat BMMSC cultures were established. Cells from each animal could be passaged for > 12 passages, with a doubling time of 24 h. CFU assay is a commonly used method to demonstrate the self-renewal and the multipotential nature of BMMSCs (Colter *et al*., 2000). Our results confirmed that the mononuclear fraction of goat cells contains the progenitor cells, which are capable of proliferation to form a detectable cluster of colonies. This property is maintained even at a higher passage (passage 7) (Fig. 2B).

Trypan blue assay revealed that cell viability was > 95% at each passage when the cells were harvested at 70% confluency. Cell viability was significantly reduced when the cells were 70% confluent (data not shown). As adherent cell cultures should be passaged when they are in the log phase before they reach confluency, an important consideration from our data is that it is imperative to passage cBMMSCs and allow them to grow at 70% confluency to maintain them at an optimal density for continued growth and to stimulate further proliferation.

Real-time PCR demonstrated that cBMMSCs were positive for CD29 (delta Ct = 0.19 ± 0.001) and CD90 (delta Ct = 2.9 ± 0.0015) and were negative for CD34 and CD45 confirming that these cells are non-hematopoietic and of mesenchymal lineage.

Finally, we examined the multipotent characteristic of cBMMSCs by assessing the *in vitro* trilineage differentiation pattern (Fig. 3). Seventy percent confluent cMSCs were induced to differentiate into each lineage. Osteogenic differentiation was confirmed at 21 days with positive alizarin red staining of calcium deposits in the differentiated cells (Fig. 3A). Chondrogenic differentiation was observed at 14 days with positive alcian blue staining of glycosaminoglycans in the differentiated cells (Fig. 3B). Additionally, adipogenic differentiation of cMSCs was confirmed at 14 days with positive oil-red-O staining of lipid molecules in the differentiated cells (Fig. 3C).

Thus, using the criteria defining MSCs (adherence to TCP, expression of cluster of differentiation markers and, finally, the potential to undergo trilineage differentiation), we confirmed that the cell cultures established from the mononuclear cells isolated from goat bone marrow were indeed adult MSCs containing osteoprogenitors and, hence, could be used as a cell source for bone tissue engineering.

Graphene and Bone Marrow-Derived Mesenchymal Stem Cell Constructs

In this study, cell adhesion, viability and proliferation assays were performed in 24-well (area: 1.9 cm^2) TCP and GO plates

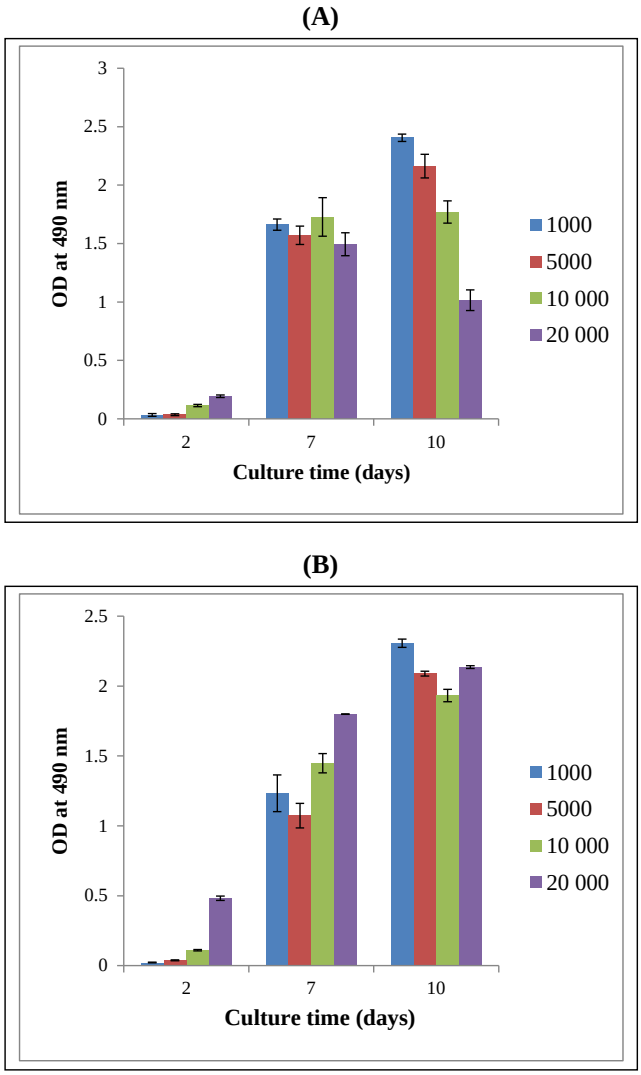

Figure 4. Comparison of proliferation of cells as determined by MTS assay for caprine bone marrow-derived mononuclear cells on polystyrene-coated tissue culture (A) and oxidized graphene (B) over a 10-day period. The results represent the means ± SD with $n = 4$ for each bar. The key denotes the number of cells used in the assay.

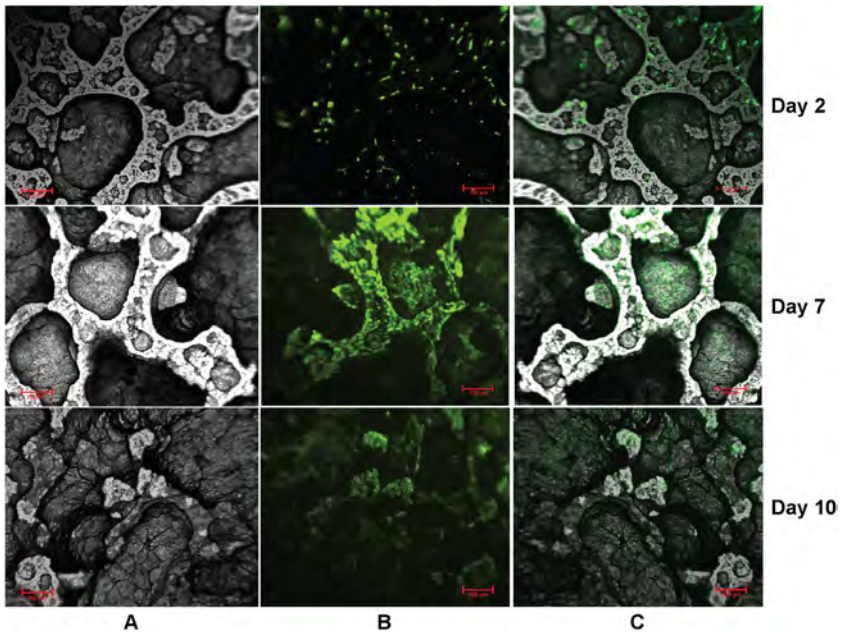

Figure 5. Cells were analyzed by calcein-AM, which exhibits green fluorescence and demonstrates live cells and propidium iodide, which displays red fluorescence and demonstrates dead cells. Fluorescent micrographs showed that over a 10-day period, cells adhered to, were viable and proliferated on oxidized graphene. Representative black and white (A), fluorescent (B) and merged (C) images are shown. Absence of red fluorescent cells indicates that oxidized graphene is not toxic to caprine bone marrow-derived mononuclear cells. Scale bar = 100 μm.

simultaneously to assess cytotoxicity of GO on cBMMSCs. The results of the cell proliferation assay demonstrated that, similar to cBMMSCs cultured on TCP, cBMMSCs seeded on GO scaffolds were able to metabolize MTS into a brown formazon product and have a high metabolic rate as a function of time (Fig. 4). Linear regression analysis of the MTS assay results for given cell numbers on TCP and GO was performed. The calculated linear regressions (R^2 values) of 1.0×10^3, 5.0×10^3, 10×10^3 and 20×10^3 cells seeded on TCP (Fig. 4A) were 0.955, 0.938, 0.769 and 0.39, respectively, indicating optimal seeding densities of 1.0×10^3 or 5.0×10^3 in the given area. By comparison, R^2 values of the same numbers of cells seeded on GO (Fig. 4B) were 0.9988, 1, 0.9318 and 0.9041, respectively, demonstrating optimal seeding densities similar to that of TCP. The lack of linear regression in cell proliferation observed when 10×10^3 and 20×10^3 are seeded on TCP is most likely due to cell death when cells become > 70% confluent. Similar results are not observed on GO surfaces. Data confirm the lack of cytotoxicity of GO on cBMMSCs.

Cell viability was further confirmed microscopically on GO using calcein-AM and propidium iodide fluorescent (live-dead) staining assay (Fig. 5). Data show that cBMMSCs seeded on GO were metabolically active, viable and, hence, grew in population over time and were well distributed throughout the GO surface.

Osteogenesis of Caprine Bone Marrow-Derived Mesenchymal Stem Cells

The osteogenic potential of cBMMSCs proliferating on GO was assessed using the cell density and differentiation cocktail found optimal in experiments described above. cBMMSCs were induced to differentiate into osteocytes, and differentiation was subjectively monitored using alizarin red staining (Fig. 6A,B) and quantitated using an osteogenic quantification assay (Fig. 6C). Data were compared between undifferentiated and differentiated cells. Data demonstrated that, unlike on TCP (Fig. 3A), alizarin red-stained bone mineralized nodules were observed at 21 days in cells proliferating on GO-coated plates in the absence of any differentiation medium. This was further confirmed by quantitation. Cells grown on GO in complete medium demonstrated two- to five-fold significantly higher alizarin red content compared to cells grown on GO in the presence of the differentiation medium (Fig. 6C) at all time points tested (days 7–21). Data suggest that graphene has a role in the differentiation of cBMMSCs toward the osteogenic lineage.

Our results are consistent with a study published by Nayak *et al.* (2011) wherein they demonstrated that, although graphene did not affect the proliferation rate of MSCs, it enhanced osteogenic differentiation of human MSCs. These findings support our hypothesis that graphene has the potential to be used as an implantable scaffold in subsequent studies of bone defects.

Given its unique 2D morphology, ability to be formed into films of controllable thickness, and its flexibility in functionalization with various chemical groups, graphene is a nanomaterial that has tremendous potential for biomedical applications in general and tissue regeneration in particular. However, further research must be conducted to understand fully the interaction of this material with various cells and tissues. In our study, GO films (hydrophilic in nature) have been proven to have an excellent ability to enhance osteogenic differentiation of cBMMSCs, indicating the part that this material could play in bone regeneration technological platforms.

Conclusions

In the present study, we demonstrated for the first time that a film formed of GO supports proliferation and osteogenic differentiation of adult MSCs isolated from goat bone marrow

Journal of Applied Toxicology

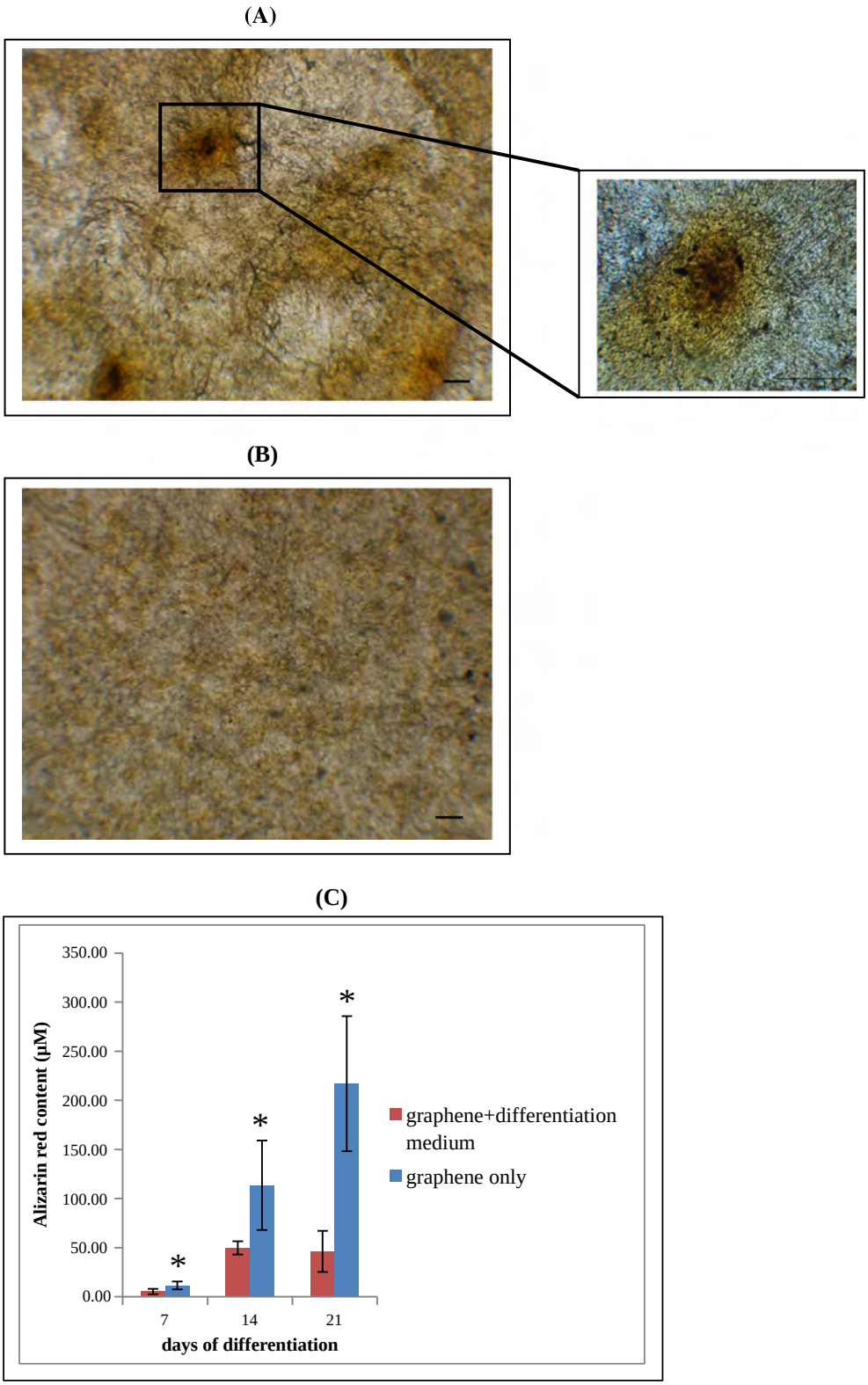

Figure 6. Osteogenic differentiation of caprine bone marrow-derived mononuclear cells on oxidized graphene (GO). Representative images showing alizarin red staining of caprine bone marrow-derived mononuclear cells seeded on GO, in presence of fetal bovine serum-containing regular growth medium (A) and osteocyte differentiation medium (B) after 21 days in culture. Note the presence of calcified nodules when cells are seeded on GO in growth media only (A). The inset shows a magnified image of the alizarin red stained calcified nodule in presence of graphene. Scale bar = 100 μm. Osteogenesis was quantitated by measuring the alizarin red content under these conditions (C). Alizarin red content (μM) in the osteocytes is graphically represented. The results represent the means ± SD with $n = 6–12$ for each bar. Alizarin red content for each sample was extrapolated from the standard curve. The key denotes the conditions used in the assay. *$P < 0.05$.

aspirates. These data exhibit *in vitro* biocompatibility and graphene's potential in bone regeneration. If these properties can be translated *in vivo*, then graphene-based nanocomposite scaffolds hold promise in bone tissue engineering.

Acknowledgments

This study was supported by the Center of Excellence in Livestock Diseases and Human Health and the Egyptian Education and Cultural Bureau. The editorial assistance of Dr. Marinelle Ringer is also acknowledged. A.S.B., E.D. and S.B acknowledge the financial support of the Food and Drug Administration/State of Arkansas program.

References

Biswas A, Bayer IS, Biris AS, Wang T, Dervishi E, Fauper F. 2012. Advances in top-down and bottom-up surface nanofabrication: techniques, applications and future prospects. *Adv. Colloid Interface Sci.* **170**: 2–27.

Bruder S, Jaiswal N, Haynesworth S. 1997. Growth kinetics, self-renewal, and the osteogenic potential of purified human mesenchymal stem cells during extensive subcultivation and following cryopreservation. *J. Cell. Biochem.* **64**: 278–294.

Carter-Arnold J, Neilsen N, Amelse L, Odoi A, Dhar M. 2013. *In vitro* analysis of equine, bone marrow-derived mesenchymal stem cells demonstrates differences within age- and gender-matched horses. *Equine Vet. J.* July 16 (Epub ahead of print). DOI: 10.1111/evj.12142.

Colter DC, Class R, DiGirolamo CM, Prockop DJ. 2000. Rapid expansion of recycling stem cells in cultures of plastic adherent cells from human bone marrow. *Proc. Natl. Acad. Sci. U. S. A.* **97**: 3213.

Dervishi E, Hategekimana F, Boyer L, Watanabe F, Mustafa T, Biswas A, Biris AR, Biris AS. 2013. The effect of carbon nanotubes and graphene on the mechanical properties of multi-component polymeric composites. *Chem. Phys. Lett.* **590**: 126–130.

Dominici M, Le Blanc K, Mueller I, Slaper-Cortenbach I, Marini F, Krause D, Deans R, Keating A, Prockop D, Horwitz E. 2006. Minimal criteria for defining multipotent mesenchymal stromal cells. The International Society for Cellular Therapy Position Statement. *Cytotherapy* **8**: 315–317.

Favi P, Benson R, Neilsen N, Hammonds R, Bates C, Stephens C, Dhar M. 2013. Cell proliferation, viability, and *in vitro* differentiation of equine mesenchymal stem cells seeded on bacterial cellulose hydrogel scaffolds. *Mater. Sci. Eng. C* **33**: 1935–1944.

Harding J, Roberts R, Mirochnitchenko O. 2013. Large animal models for stem cell therapy. *Stem Cell Res. Ther.* **4**: 23–31.

Jaiswal N, Haynesworth S, Caplan A, Bruder S. 1997. Osteogenic differentiation of purified, culture-expanded human mesenchymal stem cells *in vitro*. *J. Cell. Biochem.* **64**: 295–312.

Lee C, Wei X, Kysar JW, Hone J. 2008. Measurement of the elastic properties and intrinsic strength of monolayer graphene. *Science* **321**: 385–388.

Liu D, Yi C, Zhang D, Zhang J, Yang M. 2010. Inhibition of proliferation and differentiation of mesenchymal stem cells by carboxylated carbon nanotubes. *ACS Nano* **4**: 2185–2195.

Mahmood M, Villagarcia, H, Dervishi E, Mustafa T, Alimohammadi M, Casciano D, Khodakovskaya M, Biris AS. 2013. Role of carbonaceous nanomaterials in stimulating osteogenesis in mammalian bone cells. *J. Mater. Chem. B.* **1**: 3220–3230.

Mistry A, Mikos A. 2005. Tissue engineering strategies for bone regeneration. *Adv. Biochem. Eng. Biotechnol.* **94**: 1–22.

Murphy J, Fink D, Hunziker E, Barry F. 2003. Stem cell therapy in a caprine model of osteoarthritis. *Arthritis Rheum.* **48**: 3464–3474.

Nair MB, Varma HK, John A. 2009. Platelet-rich plasma and fibrin glue-coated bioactive ceramics enhance growth and differentiation of goat bone marrow-derived stem cells. *Tissue Eng. A.* **15**: 1619–1631.

Nandi S, Roy S, Mukherjee P, Kundu B, De D, Basu D. 2010. Orthopaedic applications of bone graft & graft substitutes: a review. *Indian J. Med. Res.* **132**: 15–30.

Nayak TR, Jian L, Phua LC, Ho HK, Ren Y, Pastorin G. 2010. Thin films of functionalized multiwalled carbon nanotubes as suitable scaffold materials for stem cells proliferation and bone formation. *ACS Nano* **4**: 7717–7725.

Nayak T, Andersen H, Makam V, Khaw C, Bae S, Xu X, Ee P, Ahn J, Hang B, Pastorin G, Ozyilmaz B. 2011. Graphene for controlled and accelerated osteogenic differentiation of human mesenchymal stem cells. *ACS Nano* **5**: 4670–4678.

Park J, Park S, Ryu S, Bhang SH, Kim J, Yoon JK, Park YH, Cho SP, Lee S, Hong BH, Kim BS. 2013. Graphene-regulated cardiomyogenic differentiation process of mesenchymal stem cells by enhancing the expression of extracellular matrix proteins and cell signaling molecules. *Adv. Healthc. Mater.* Aug 15. (Epub ahead of print) DOI: 10.1002/adhm.201300177.

Pittenger M, Mackay A, Beck S, Jaiswal R. 1999. Multilineage potential of adult human mesenchymal stem cells. *Science* **284**: 143–147.

Pruneanu S, Biris AR, Pogacean F, Lazar DM, Ardelean S, Watanabe F, Dervishi E, Biris AS. 2012. Novel multifunctional graphene sheets with encased Au/Ag nanoparticles for advanced electrochemical analysis of organic compounds. *Chemphyschem* **13**: 3632–3629.

Ren Y, Wu H, Zhou X, Wen J, Jin M, Cang M, Guo X, Wang Q, Liu D, Ma Y. 2012. Isolation, expansion, and differentiation of goat adipose-derived stem cells. *Res. Vet. Sci.* **93**: 404–411.

Salgado A, Coutinho O, Reis R. 2004. Bone tissue engineering: state of the art and future trends. *Macromol. Biosci.* **4**: 743–765.

Tang T, Lu B, Yue B, Xie X, Xie Y, Dai K. 2007. Treatment of osteonecrosis of the femoral head with hBMP-2-gene-modified tissue-engineered bone in goats. *J. Bone Joint Surg. Br.* **89**: 127–129.

Zhang L, Wang Z, Xu C, Li Y, Gao J, Wang W, Liu Y. 2011. High strength graphene oxide/polyvinyl alcohol composite hydrogels. *J. Mater. Chem.* **21**: 10399–10406.

Zhao C, Tan A, Pastorin G, Ho H. 2013. Nanomaterial scaffolds for stem cell proliferation and differentiation in tissue engineering. *Biotechnol. Adv.* **31**: 654–668.